

# Fast macromolecular proton fraction mapping from a single off-resonance magnetization transfer measurement

V. L. Yarnykh<sup>1</sup>

<sup>1</sup>Radiology, University of Washington, Seattle, WA, United States

**Introduction:** Cross-relaxation imaging (CRI) is a new quantitative MRI method, which allows the measurement and *in vivo* mapping of key parameters determining magnetization transfer (MT) between water and macromolecules in tissues (1,2). One of these parameters, macromolecular proton fraction (MPF, also termed bound pool fraction) is of special interest, since it provides direct measurement of the portion of macromolecular protons causing the MT effect and is indicative of the total content of macromolecules in tissues. While all parameters of the two-pool model (specifically, the MPF  $f$ ; the rate constant  $k$ , and the transverse relaxation times of the free and bound pools  $T_2^F$  and  $T_2^B$ ) can be determined using an appropriate CRI experimental design with a sufficiently large number of measurements (3-5), recent studies have been focused on the development of faster acquisition techniques allowing determination of subsets of two-pool model parameters from a limited number of experimental points based on certain theoretical approximations (2-4). Recently, a time-efficient methodology for single-parameter MPF mapping from two off-resonance MT measurements has been proposed (4) based on constraining other model parameters (specifically,  $T_2^B$ , the product  $T_2^F R_1^F$ , and the inverse rate constant  $R=k(1-f)/f$ ) with their average-brain values. In this study, we demonstrate the feasibility of further reduction of the scan time for MPF mapping by utilizing only one off-resonance point and characterize the accuracy of this approach.

**Methods:** **Subjects:** Data were obtained from two healthy controls (female, age 45 and 49 years) and two relapsing-remitting multiple sclerosis (MS) patients (female, age 33 and 52 years) in accordance with local IRB regulations. **MRI protocol:** Subjects were imaged at 3.0 T (Philips Achieva, Best, Netherlands) with a transmit/receive head coil. 21 pulsed Z-spectroscopic data points with variable offset frequencies ( $\Delta$ ) of the off-resonance saturation pulse ( $\Delta = 0.6, 1, 2, 4, 8, 12$ , and 16 kHz) and effective flip angles ( $FA_{MT}=600^\circ, 800^\circ$ , and  $980^\circ$ ) were acquired with a 3D spoiled MT-prepared gradient echo (GRE) pulse sequence (TR/TE = 43/2.3 ms,  $\alpha = 10^\circ$ , single-lobe sinc saturation pulse with duration 19 ms). A reference image for data normalization was obtained with  $\Delta=96$  kHz (no MT effect is observed at this frequency) for each effective flip angle to ensure that the transmitter operates with identical gain settings. A complementary  $R_1$  map necessary for parameter fitting was obtained using the variable flip angle (VFA) method with a 3D spoiled GRE sequence (TR/TE = 20/2.3 ms,  $\alpha = 3, 10$ , and  $20^\circ$ ). All Z-spectroscopic and VFA images were acquired with FOV = 240×180×120 mm, matrix

= 160×120×24, resolution 1.5×1.5×5.0 mm (zero-interpolated to 1.0×1.0×2.5 mm), and one signal average. Scan time was 1 min 30 s and 43 s per point for Z-spectroscopy and VFA, respectively. To correct for effects of  $B_0$  and  $B_1$  heterogeneity, whole-brain  $B_0$  and  $B_1$  maps were acquired using previously described techniques (6,7). **Image processing:** The reference standard for  $f$  maps was obtained from 4-parameter fitting ( $k, f, T_2^F$ , and  $T_2^B$ ) of the matrix pulsed MT model (2) using 21-point data and a complementary  $R_1$  map with  $B_0$  and  $B_1$  correction similar to the previously described procedure (3,4). To test the proposed single-point method,  $f$  maps were reconstructed by iterative solution of the nonlinear matrix MT equation (2) using Gauss-Newton method for each data point. The constraints for the parameters  $R$ ,  $T_2^B$ , and  $T_2^F R_1^F$  were determined as described below. The root-mean-square error ( $\sigma_f$ ) was calculated in each voxel between reference and single-point  $f$  maps and then normalized to the total number of voxels. After reconstruction of MPF maps, the brain was segmented, and normalized parametric histograms were computed. **Simulations:** To find optimal sampling conditions, the error model was created based on the error propagation theory. In brief, the RMS error of the parameter  $f$  ( $\sigma_f$ ) is described by the sum of terms reflecting the variance due to noise in source images and bias due to potential deviation of constrained parameters from their true values.

**Results:** **Validation using the full-model fit:** The maps of the parameters constrained during single-parameter single-point  $f$  reconstruction ( $R$ ,  $T_2^B$ , and the product  $T_2^F R_1^F$ ) demonstrate very minor tissue-dependent variations (Fig. 1) thus supporting the rationale of using their fixed values for fast MPF mapping. Of note, variability of the parameters  $R$  and  $T_2^F R_1^F$  is mostly associated with interfaces between gray matter (GM) and CSF, where the four-parameter fit becomes unreliable. Tissue-dependent variations of  $T_2^B$  appear to be related to fiber directionality in white matter (WM) that is a new finding, though its detailed interpretation is beyond the scope of this study. Whole-brain histograms of these parameters (Fig. 2a-c) exhibit unimodal distributions, which are very similar for MS patients and controls. To alleviate the effect of outlying voxels, median values (instead of mean) were measured from histograms and used as average-brain constraints, resulting in the following parameter set:  $R=19$  s<sup>-1</sup>,  $T_2^B=9.5$   $\mu$ s, and  $T_2^F R_1^F=0.022$ . MPF maps reconstructed by both techniques (four-parameter fit and single-parameter iterative solution for an optimal sampling point as discussed below) demonstrate very close agreement (Fig. 1). MPF histograms (Fig. 2d) are characterized by a bimodal shape, where two peaks correspond to GM (mode 6.8% for controls and 6.3% for MS patients) and WM (mode 13.5% for controls and 12.8% for MS patients). The shapes of MPF histograms produced by both reconstruction techniques appear essentially similar. Notably, the distinctions between MS patients and controls are manifested in MPF histograms as a clearly visible shift of the WM peak and a less prominent shift of the GM peak to lower MPF values. This trend is completely preserved by the single-point single-parameter reconstruction method. **Error analysis and sampling optimization:** The theoretical error propagation model appears in a good agreement with experimental data (Fig. 3). Both theory and experiment suggest that MPF measurement error depends on the offset frequency and flip angle settings. For the particular sequence parameters, the best MPF accuracy is achieved if the sampling point  $\Delta$  is chosen in 4-6 kHz range. There is also an optimum for the saturation flip angle (data not shown), which is achieved in a range of  $FA_{MT}=600^\circ$ - $700^\circ$ . Accordingly, the experimental data for  $\Delta=4$  kHz and  $FA_{MT}=600^\circ$  described above correspond to nearly optimal sampling conditions. At these conditions, the absolute MPF RMS error per voxel is  $\sim 0.7\%$  (Fig. 3), which translates into  $\sim 5$ - $10\%$  relative errors for a range of physiological MPF values.

**Conclusions:** This study demonstrates the feasibility of fast and accurate MPF mapping using only a single-offset MT-weighted image. This approach is the fastest to date quantitative MT (qMT) method, which requires no extra time compared to traditional magnetization transfer ratio (MTR) mapping, if a complementary  $T_1$  map is available. Since the proposed method rapidly determines MPF with high accuracy, it provides a viable alternative to both time-consuming multi-parameter qMT techniques and fast but poorly-interpretable MTR measurements.

**References:** (1) Yarnykh VL. *MRM* 2002;47:929. (2) Yarnykh VL, Yuan C. *Neuroimage* 2004;23:409. (3) Underhill HR, et al. *Neuroimage* 2009;47:1568. (4) Underhill HR, et al. *Neuroimage* 2010; In press. (5) Sled JG, Pike GB. *MRM* 2001; 46:923. (6) Skinner TE, Glover GH. *MRM* 1997;37:628. (7) Yarnykh VL. *MRM* 2007;57:192.

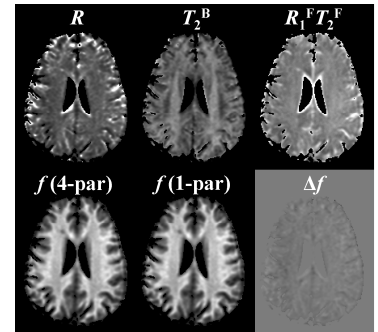


**Fig 1.** Example parametric maps obtained from an MS patient. **Top row:** actual maps of the parameters constrained during single-parameter single-point  $f$  reconstruction ( $R$ ,  $T_2^B$ , and the product  $T_2^F R_1^F$ ). **Bottom row:** MPF ( $f$ ) maps obtained by the four-parameter fit of the 21-point dataset and by the single-parameter single-point ( $\Delta=4$  kHz,  $FA_{MT}=600^\circ$ ) iterative solution, and their difference image ( $\Delta f$ ). The difference image is presented with the same window width as  $f$  maps.

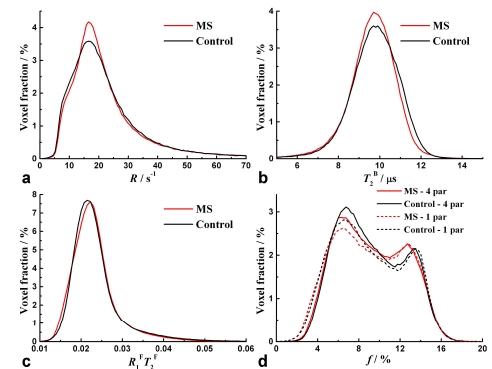


**Fig 2.** Average group (MS and controls) whole-brain histograms of the parameters constrained during single-parameter single-point  $f$  reconstruction ( $R$  (a),  $T_2^B$  (b), and the product  $T_2^F R_1^F$  (c)) and comparison of MPF histograms (d) computed from  $f$  maps obtained by the four-parameter fit of 21-point datasets and by the single-parameter single-point ( $\Delta=4$  kHz,  $FA_{MT}=600^\circ$ ) iterative solution.

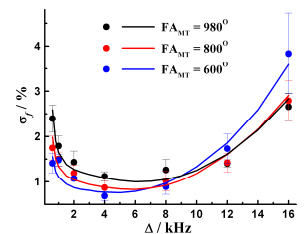


**Fig. 3.** Experimental (points) and simulated (lines) RMS error in MPF ( $\sigma_f$ ) as a function of the offset frequency for different saturation flip angles.